Journal of Engineering Mathematics **44:** 1–20, 2002.

A state of stress and displacement of elastic plates using simple and mixed shear deformation theories

A.M. ZENKOUR
Department of Mathematics, Faculty of Education, Tanta University, Kafr El-Sheikh 33516, Egypt
(e-mail: Zenkour@edu-kaf.edu.eg)

Received 17 April 2001; accepted in revised form 15 November 2001

Abstract. This paper presents accurate two-dimensional solutions for bending response of four types of single-layer orthotropic rectangular plates. The plates considered are of the type having two opposite sides simply-supported, and two other sides having combinations of simply-supported, clamped, and free-boundary conditions. Analytical solutions for deflections and stresses of rectangular plates are developed by means of the simple (SFPT) and mixed (MFPT) first-order shear deformable plate theories. The present MFPT not only shows improvement on predicting frequencies, critical buckling loads, deflections and in-plane stresses, but also accounts for variable transverse shear stress distributions through the thickness. This puts into evidence the important role played by MFPT in the modeling of homogeneous plate theories, which in contrast to SFPT does not require the incorporation of a shear-correction factor. For illustrative purposes, sample free vibration, stability, and bending problems for simply supported orthotropic plates are considered and comparisons of the obtained results are made with the exact and higher-order shear deformation theory results given in the literature.

Key words: bending response, orthotropic plates, shear correction factors.

1. Introduction

Classical plate theory has been widely used in static and dynamic analysis of relatively thin plates, but it is not suitable for thick plates and laminates [1–3]. This theory, as some of the theories for moderately thick plates, comprises the assumption that the transversal normal stresses vanish identically. The relation between the longitudinal normal stresses and corresponding relative deformations is derived from this assumption. In these theories the influence of the transversal distribution of the loading is ignored; the load is reduced to the mid-plane and the transversal deflection is constant for all points on a normal to the mid-plane.

The simple first-order transverse shear deformation plate theory (SFPT) [4–7] proposed by Reissner [4, 5] and Mindlin [6] assumes that the in-plane displacements are linear and the transverse deflection is constant through the thickness. It results in a fairly accurate global response for isotropic materials when used with an appropriate shear-correction factor, even though parabolic transverse shear strain distributions through the thickness are not described. Yang *et al.* [8] extended the SFPT to laminated plates, followed by many variants of the first-order theory. Reissner [9], Noor and Burton [10], and Reddy [11] have reviewed these developments.

Many theories have been developed to overcome the deficiency of SFPT, namely constant or uniform transverse shear strain distributions through the thickness. Whitney and Sun [12] proposed a second-order theory, which allows linear variations of transverse shear strains through the thickness. Various third-order theories that lead to parabolic distributions

of transverse shear strains through the thickness have also been developed [13–16]. Reddy's third-order shear deformation plate theory [14, 15] allows for a quadratic distribution of transverse shearing strain through the thickness of the plate by assuming a cubic expansion of the in-plane displacements in the thickness coordinate. The form of the assumed displacement functions is simplified by enforcing traction-free boundary conditions at the top and bottom surfaces of the plate. No shear-correction factors are needed, because a correct representation of the transverse shearing strain is given. The first- and third-order plate theories contain the same number of dependent variables, but the one that is variationally consistent with Reddy's theory involves additional higher-order stress resultants and material stiffness coefficients compared to the first-order theory.

It is possible to obtain closed-form solutions in a few exceptional cases of a 3D analysis of plates and cylinders. The first solutions of this type were presented by Srinivas and Rao [17], Pagano [18, 19], and Pagano and Hatfield [20]. Srinivas and Rao [17] have exactly investigated the bending, vibration and buckling of simply supported thick orthotropic rectangular plates and laminates based on a 3D-elasticity theory. A comparison of numerical results of Mindlin's plate theory and the classical plate theory has been given. Pagano [18, 19] has developed exact solutions for laminated plates and compared them with the results for the classical laminated plate theory. Pagano and Hatfield [20] have considered the response of multi-ply laminates with a view toward examining the generality of previous conclusions regarding the range of validity of the classical theory for laminated plates.

The first-order shear deformation theory is still the most attractive approach due to its simplicity and low computational cost. It is well recognized that, while SFPT is adequate for global structural behaviour (*e.g.* transverse deflections, fundamental vibration frequencies, critical buckling loads, force and moment resultants), it is not adequate for accurate prediction of local response parameters, such as the interlaminar stress distributions wherein the transverse shear strains derived from the displacement field assumptions are evenly distributed or uniform through the thickness.

In a very recent paper [21], a relationship between the simple and mixed first-order transverse shear deformation theories is presented. Analytical solutions for natural frequencies and buckling loads of anisotropic plates under various boundary conditions are developed. The mixed first-order transverse shear-deformation plate theory (MFPT) is a modification of the SFPT. It retains the basic displacement assumptions of Reissner-Mindlin's traditional SFPT (*i.e.* the in-plane displacements vary linearly and the transverse displacement is constant through the thickness). In the MFPT, both the displacements and stresses must be considered as arbitrary. For this reason a mixed variational formulation should be used [21–25]. The MFPT is developed based on a mixed variational formulation which assumes continuous stress distributions through the plate thickness. Also, the transverse shear stresses are consistent with the surface conditions. So, the rationale for the shear-correction factor required for the SFPT is obviated. In addition, the effect of transverse normal stress is taken into account.

In the present paper, the simple and mixed shear deformation theories are used to solve the bending problem of single-layer orthotropic plates under various boundary conditions. The plate edges $y = 0, b$ are assumed to be simply-supported, while the remaining ones, $x = 0, a$, have arbitrary combinations of edge conditions. Numerical results of deflections and stresses of orthotropic flat plates are presented. Sample problems for natural frequencies and critical buckling loads are also presented. As in the author's previous paper [21], the variational approach is applicable to SS, CC, CS and CF plates (where S is simply-supported, C is clamped, and F is free). Comparisons with some of the available results (obtained for

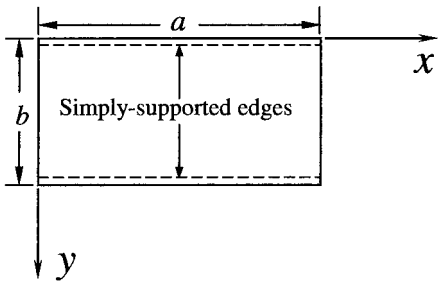

Figure 1. Geometry and coordinate system of rectangular plate ($a \times b$).

simply-supported edge conditions) are undertaken and appropriate conclusions concerning the various effects are formulated. The MFPT not only accounts for the correct through-the-thickness transverse shear stress distributions, but also satisfies pointwise all the equilibrium equations, constitutive relations and boundary conditions for the orthotropic plates.

2. Derivation of governing equations

Consider a rectangular plate of length a, width b and uniform thickness h. The mid-plane of the plate will be taken as the xy plane, and the x and y axes are directed along the edges (see Figure 1). The z-axis is taken perpendicular to the mid-plane and positive in a downward direction. A normal traction $f(x, y)$ is applied on the upper surface, while the lower surface is traction-free. Also, the in-plane edge farces S_1 and S_2 are applied in the directions x and y, respectively, and are considered positive in tension.

The strain-displacement relations for the first-order theory are given immediately as

$$\varepsilon_{ij}^{\alpha} = \overline{\varepsilon}_{ij}^{\alpha} + z\kappa_{ij}^{\alpha}, \quad \varepsilon_{j3}^{\alpha} = \overline{\varepsilon}_{j3}^{\alpha}, \quad \varepsilon_{33}^{\alpha} = 0, \quad (i, j = 1, 2), \tag{2.1}$$

where

$$\begin{aligned} &\overline{\varepsilon}_{11}^{\alpha} = \frac{\partial u^{\alpha}}{\partial x}, \quad \overline{\varepsilon}_{22}^{\alpha} = \frac{\partial v^{\alpha}}{\partial y}, \quad \overline{\varepsilon}_{23}^{\alpha} = \varphi^{\alpha} + \frac{\partial w^{\alpha}}{\partial y}, \quad \overline{\varepsilon}_{13}^{\alpha} = \psi^{\alpha} + \frac{\partial w^{\alpha}}{\partial x}, \\ &\overline{\varepsilon}_{12}^{\alpha} = \frac{\partial v^{\alpha}}{\partial x} + \frac{\partial u^{\alpha}}{\partial y}, \quad \kappa_{11}^{\alpha} = \frac{\partial \psi^{\alpha}}{\partial x}, \quad \kappa_{22}^{\alpha} = \frac{\partial \varphi^{\alpha}}{\partial y}, \quad \kappa_{12}^{\alpha} = \frac{\partial \varphi^{\alpha}}{\partial x} + \frac{\partial \psi^{\alpha}}{\partial y}, \end{aligned} \tag{2.2}$$

in which $(u^{\alpha}, v^{\alpha}, w^{\alpha})$ denote the displacements of a point (x, y) on the mid-plane, and ψ^{α} and φ^{α} are the rotations of normals to mid-plane about the y and x axes, respectively. Note that quantities with superscript '$\alpha = \mathrm{S}$' refer to the SFPT, while quantities with '$\alpha = \mathrm{M}$' refer to the MFPT.

For SFPT the stress-strain relations of an orthotropic body are given by:

$$\begin{Bmatrix} \sigma_{11}^{\mathrm{S}} \\ \sigma_{22}^{\mathrm{S}} \\ \sigma_{23}^{\mathrm{S}} \\ \sigma_{13}^{\mathrm{S}} \\ \sigma_{12}^{\mathrm{S}} \end{Bmatrix} = \begin{bmatrix} c_{11} & c_{12} & 0 & 0 & 0 \\ c_{12} & c_{22} & 0 & 0 & 0 \\ 0 & 0 & c_{44} & 0 & 0 \\ 0 & 0 & 0 & c_{55} & 0 \\ 0 & 0 & 0 & 0 & c_{66} \end{bmatrix} \begin{Bmatrix} \varepsilon_{11}^{\mathrm{S}} \\ \varepsilon_{22}^{\mathrm{S}} \\ \varepsilon_{23}^{\mathrm{S}} \\ \varepsilon_{13}^{\mathrm{S}} \\ \varepsilon_{12}^{\mathrm{S}} \end{Bmatrix}, \tag{2.3}$$

in which c_{ij} are the reduced stiffnesses, see the monograph of Whitney [3, Chapter 1]. Note that the transverse normal stress σ_{33}^{S} is dropped.

For MFPT, the final expressions for the stress components can be written in terms of their resultants and the thickness coordinate z [21]:

$$\begin{aligned}
&\sigma_{pq}^{\mathrm{M}} = \frac{N_{pq}^{\mathrm{M}}}{h} + \frac{12M_{pq}^{\mathrm{M}}}{h^3}z, \quad \sigma_{p3}^{\mathrm{M}} = \frac{3Q_{p3}^{\mathrm{M}}}{2h}\left[1-\left(\frac{z}{h/2}\right)^2\right], \\
&\sigma_{33}^{\mathrm{M}} = \frac{f}{4}\left[1-2\left(\frac{z}{h/2}\right)-5\left(\frac{z}{h/2}\right)^2\right]\left(1-\frac{z}{h/2}\right), \quad (p,q=1,2).
\end{aligned} \tag{2.4}$$

It should be noted that the transverse shear stresses σ_{13}^{M} and σ_{23}^{M} are functions of z and vanish on the bounding planes ($z = \pm h/2$). In addition, the transverse normal stress σ_{33}^{M} satisfies the following conditions:

$$\sigma_{33}^{\mathrm{M}}\big|_{z=-h/2} = -f, \quad \sigma_{33}^{\mathrm{M}}\big|_{z=+h/2} = 0, \quad \int_{-h/2}^{+h/2}\sigma_{33}^{\mathrm{M}}\,\mathrm{d}z = 0, \quad \int_{-h/2}^{+h/2} z\sigma_{33}^{\mathrm{M}}\,\mathrm{d}z = 0. \tag{2.5}$$

The stress resultants for SFPT and MFPT are given by:

$$\begin{aligned}
&\left\{N_{pq}^{\alpha}, M_{pq}^{\alpha}\right\} = \int_{-h/2}^{+h/2}\sigma_{pq}^{\alpha}\{1,z\}\,\mathrm{d}z, \\
&Q_{p3}^{\alpha} = \int_{-h/2}^{+h/2} K_p^{\alpha}\sigma_{p3}^{\alpha}\,\mathrm{d}z, \ (p,q=1,2),
\end{aligned} \tag{2.6}$$

where $K_p^{\mathrm{S}}(K_1^{\mathrm{S}} = K_2^{\mathrm{S}} = k)$ are shear factors appearing in Reissner-Mindlin's traditional SFPT used to correct for the errors stemming from (2.3) that σ_{13}^{S} and σ_{23}^{S} are constants over the thickness of the plate (*i.e.*, are not functions of z). Note that there is no need for shear correction factors to MFPT (*i.e.*, $K_p^{\mathrm{M}} = 1$).

2.1. Equation of motion

The simple and mixed variational formulations based upon Hamilton's principle are given, respectively, by (see, *e.g.*, [21–24]):

$$0 = \int_{t_1}^{t_2}\left[\iiint_V \left(\rho\ddot{u}_i^{\mathrm{S}}\delta u_i^{\mathrm{S}} + \delta U^{\mathrm{S}}\right)\,\mathrm{d}v + \delta\Pi^{\mathrm{S}}\right]\mathrm{d}t, \tag{2.7}$$

$$0 = \int_{t_1}^{t_2}\left[\iiint_V \left(\rho\ddot{u}_i^{\mathrm{M}}\delta u_i^{\mathrm{M}} + \delta(\sigma_{ij}^{\mathrm{M}}\varepsilon_{ij}^{\mathrm{M}} - R^{\mathrm{M}})\right)\mathrm{d}v + \delta\Pi^{\mathrm{M}}\right]\mathrm{d}t, \tag{2.8}$$

where (t_1, t_2) is a time interval; ρ is the density of the undeformed body; U^{S} is the strain-energy density,

$$U^{\mathrm{S}} = \frac{1}{2}[c_{11}(\varepsilon_{11}^{\mathrm{S}})^2 + c_{22}(\varepsilon_{22}^{\mathrm{S}})^2 + c_{44}(\varepsilon_{23}^{\mathrm{S}})^2 + c_{55}(\varepsilon_{13}^{\mathrm{S}})^2 + c_{66}(\varepsilon_{12}^{\mathrm{S}})^2] + c_{12}\varepsilon_{11}^{\mathrm{S}}\varepsilon_{22}^{\mathrm{S}}, \tag{2.9}$$

and R^{M} is the complementary energy density,

$$\begin{aligned}
R^{\mathrm{M}} = {} & \frac{1}{2}\left[a_{11}(\sigma_{11}^{\mathrm{M}})^2 + a_{22}(\sigma_{22}^{\mathrm{M}})^2 + a_{33}(\sigma_{33}^{\mathrm{M}})^2 + a_{44}(\sigma_{23}^{\mathrm{M}})^2 + a_{55}(\sigma_{13}^{\mathrm{M}})^2 + a_{66}(\sigma_{12}^{\mathrm{M}})^2\right] \\
& + a_{12}\sigma_{11}^{\mathrm{M}}\sigma_{22}^{\mathrm{M}} + a_{23}\sigma_{22}^{\mathrm{M}}\sigma_{33}^{\mathrm{M}} + a_{13}\sigma_{11}^{\mathrm{M}}\sigma_{33}^{\mathrm{M}},
\end{aligned} \tag{2.10}$$

which a_{ij} are the strain coefficients (compliances). The potential energy $\Pi^{\alpha}(\alpha = \mathrm{S}, \mathrm{M})$ of the applied loads can be defined as a function of the displacement field u_i^{α} and the applied loads as follows:

$$\Pi^{\mathrm{S}} = -\iiint_V B_i u_i^{\mathrm{S}} \, \mathrm{d}v - \iint_{S\sigma} \overline{F}_i u_i^{\mathrm{S}} \, \mathrm{d}s, \tag{2.11}$$

$$\Pi^{\mathrm{M}} = -\iiint_V B_i u_i^{\mathrm{M}} \, \mathrm{d}v - \iint_{S\sigma} \overline{F}_i u_i^{\mathrm{M}} \, \mathrm{d}s - \iint_{Su} n j \sigma_{ij}^{\mathrm{M}}(\overline{u}_i^{\mathrm{M}}) \, \mathrm{d}s, \tag{2.12}$$

where n_j are the components of the unit vector along the outward normal to the total surface $S_\sigma + S_u$; B_i are the body forces measured per unit volume of the undeformed body; $\overline{F}_i$ are the prescribed components of the stress vector, per unit area of the surface $S\sigma$ and $\overline{u}_i^{\mathrm{M}}$ are the prescribed components of the displacements of the remaining surface S_u. In the absence of body forces and the prescribed displacements, we have for the first variation of Π^{α},

$$\delta\Pi^{\alpha} = \iint_{S_\sigma} \left(S_1 \frac{\partial w^{\alpha}}{\partial x} \frac{\partial}{\partial x} + S_2 \frac{\partial w^{\alpha}}{\partial y} \frac{\partial}{\partial y} - f \right) \delta w^{\alpha} \, \mathrm{d}s. \tag{2.13}$$

The next step in deriving the governing equations consists of the substitution of Equations (2.1), (2.3), (2.4), (2.9), (2.10), and (2.13) in the variational formulations (2.7) and (2.8). The extremum conditions give the following dynamic equations:

$$\begin{aligned}
&\frac{\partial N_{11}^{\alpha}}{\partial x} + \frac{\partial N_{12}^{\alpha}}{\partial y} = \rho h \ddot{u}^{\alpha}, \quad \frac{\partial N_{12}^{\alpha}}{\partial x} + \frac{\partial N_{22}^{\alpha}}{\partial y} = \rho h \ddot{v}^{\alpha}, \\
&\frac{\partial Q_{13}^{\alpha}}{\partial x} + \frac{\partial Q_{23}^{\alpha}}{\partial y} + f + \frac{\partial}{\partial x}\left(S_1 \frac{\partial w^{\alpha}}{\partial x} \right) + \frac{\partial}{\partial y}\left(S_2 \frac{\partial w^{\alpha}}{\partial y} \right) = \rho h \ddot{w}^{\alpha}, \\
&\frac{\partial M_{11}^{\alpha}}{\partial x} + \frac{\partial M_{12}^{\alpha}}{\partial y} - Q_{13}^{\alpha} = \rho \frac{h^3}{12} \ddot{\psi}^{\alpha}, \quad \frac{\partial M_{12}^{\alpha}}{\partial x} + \frac{\partial M_{22}^{\alpha}}{\partial y} - Q_{23}^{\alpha} = \rho \frac{h^3}{12} \ddot{\varphi}^{\alpha}.
\end{aligned} \tag{2.14}$$

2.2. Boundary conditions

The form of the geometric and force boundary conditions is also given below:

Geometric (essential)	Force (natural)
u^{α}	$N_{11}^{\alpha} n_x + N_{12}^{\alpha} n_y$
v^{α}	$N_{12}^{\alpha} n_x + N_{22}^{\alpha} n_y$
w^{α}	$\left(Q_{13}^{\alpha} + S_1 \frac{\partial w^{\alpha}}{\partial x} \right) n_x + \left(Q_{23}^{\alpha} + S_2 \frac{\partial w^{\alpha}}{\partial y} \right) n_y$
ψ^{α}	$M_{11}^{\alpha} n_x + M_{12}^{\alpha} n_y$
φ^{α}	$M_{12}^{\alpha} n_x + M_{22}^{\alpha} n_y$

In which (n_x, n_y) denote the direction cosines of a unit normal to the boundary of the midplane.

2.3. Constitutive equations

For the SFPT, the stress resultants are related to the strains by Equation (2.3), while for the MFPT they will be derived from the extremum condition of the mixed variational formulation (2.8). In general, the constitutive equations are given by:

$$
\begin{aligned}
&N^{\alpha}_{11} = A^{\alpha}_{11}\overline{\varepsilon}^{\alpha}_{11} + A^{\alpha}_{12}\overline{\varepsilon}^{\alpha}_{22}, \quad N^{\alpha}_{22} = A^{\alpha}_{12}\overline{\varepsilon}^{\alpha}_{11} + A^{\alpha}_{22}\overline{\varepsilon}^{\alpha}_{22},\\
&M^{\alpha}_{11} = D^{\alpha}_{11}\kappa^{\alpha}_{11} + D^{\alpha}_{12}\kappa^{\alpha}_{22}, \quad M^{\alpha}_{22} = D^{\alpha}_{12}\kappa^{\alpha}_{11} + D^{\alpha}_{22}\kappa^{\alpha}_{22},\\
&N^{\alpha}_{12} = A^{\alpha}_{66}\overline{\varepsilon}^{\alpha}_{12}, M^{\alpha}_{12} = D^{\alpha}_{66}\kappa^{\alpha}_{12}, Q^{\alpha}_{23} = A^{\alpha}_{44}\overline{\varepsilon}^{\alpha}_{23}, Q^{\alpha}_{13} = A^{\alpha}_{55}\overline{\varepsilon}^{\alpha}_{13},
\end{aligned}
\tag{2.15}
$$

where

$$
\begin{bmatrix} A^{\mathrm{M}}_{11} & A^{\mathrm{M}}_{12} \\ A^{\mathrm{M}}_{12} & A^{\mathrm{M}}_{22} \end{bmatrix} = h \begin{bmatrix} a_{11} & a_{12} \\ a_{12} & a_{22} \end{bmatrix}^{-1}, \quad A^{\mathrm{M}}_{rr} = \frac{5h}{6a_{rr}}, \quad A^{\mathrm{M}}_{66} = \frac{h}{a_{66}},
\tag{2.16}
$$

$$
A^{\mathrm{S}}_{rr} = hkc_{rr}, \quad A^{\mathrm{S}}_{pq} = hc_{pq}, \quad D^{\alpha}_{pq} = \frac{h^2}{12}A^{\alpha}_{pq}, \quad (r = 4, 5;\ p, q = 1, 2, 6).
$$

For an orthotropic body the elastic constants c_{ij} and compliances a_{ij} may be expressed in terms of the engineering orthotropic characteristics (Young's moduli E_i, shear moduli G_{ij} and Poisson's ratios v_{ij}) as:

$$
\begin{aligned}
&c_{11} = \frac{E_1}{1 - v_{12}v_{21}}, \quad c_{12} = \frac{E_2 v_{12}}{1 - v_{12}v_{21}} = \frac{E_1 v_{21}}{1 - v_{12}v_{21}}, \ c_{22} = \frac{E_2}{1 - v_{12}v_{21}}, \ c_{44} = G_{23} = \frac{1}{a_{44}},\\
&c_{55} = G_{13} = \frac{1}{a_{55}}, \quad c_{66} = G_{12} = \frac{1}{a_{66}}, \quad a_{11} = \frac{1}{E_1}, \quad a_{12} = -\frac{v_{12}}{E_1} = -\frac{v_{21}}{E_2}, \quad a_{22} = \frac{1}{E_2}.
\end{aligned}
\tag{2.17}
$$

3. Solutions procedure

The simple and mixed variational formulations will be extended here in order to analyze the free vibration, buckling, and bending problems of rectangular plates. The SFPT and MFPT will be established in this section by suppressing the in-plane displacement degree of freedom. Further, we will assume, as shown in Figure 1, that two opposite edges of the plate at $y = 0$ and b are invariably simply-supported (*i.e.*, $w^{\alpha} = \psi^{\alpha} = M^{\alpha}_{22} = 0$). At the other two edges of the plate, $x = 0$ and a, we can have a combination of the following cases:

S (Simply-supported edge):

$$
w^{\alpha} = \varphi^{\alpha} = M^{\alpha}_{11} = 0,
\tag{3.1}
$$

C (Clamped edge):

$$
w^{\alpha} = \psi^{\alpha} = \varphi^{\alpha} = 0,
\tag{3.2}
$$

F (Free edge):

$$
M^{\alpha}_{11} = M^{\alpha}_{12} = Q^{\alpha}_{13} + S_1\frac{\partial w^{\alpha}}{\partial x} = 0.
\tag{3.3}
$$

The following representation for the displacement quantities (deleting stretching effects) is appropriate in the analysis of all problems:

$$
\begin{Bmatrix} w^{\alpha} \\ \psi^{\alpha} \\ \varphi^{\alpha} \end{Bmatrix} = \sum_{n=1}^{N} \begin{Bmatrix} W^{\alpha}_n \ \sin\ \mu_n y \\ \Psi^{\alpha}_n \ \sin\ \mu_n y \\ \Phi^{\alpha}_n \ \cos\ \mu_n y \end{Bmatrix} \mathrm{e}^{i\omega t},
\tag{3.4}
$$

where ω denotes the eigenfrequency and $\mu_n = n\pi/b$. The above solution satisfies the simply-supported boundary condition at $y = 0$ and $y = b$. Similarly, the load f is represented as

$$f(x, y) = \sum_{n=1}^{N} F_n(x) \sin \mu_n y. \tag{3.5}$$

For various distributions of $f(x, y)$ and various boundary conditions, the coefficients F_n are given by

$$F_n = \frac{4f_0}{n\pi}, \quad n = 1, 3, 5, \ldots, N, \tag{3.6}$$

where f_0 represents the intensity of the load at the center of the plate.

In the general case in which F_n is an arbitrary function of x, the particular solution is determined by expanding the solution (3.4) in a Fourier series

$$\begin{Bmatrix} W_n^\alpha \\ \Psi_n^\alpha \\ \Phi_n^\alpha \end{Bmatrix} = \sum_{m=1}^{N} \begin{Bmatrix} W_{mn}^\alpha X(\lambda_m x) \\ \Psi_{mn}^\alpha X'(\lambda_m x) \\ \Phi_{mn}^\alpha X(\lambda_m x) \end{Bmatrix}, \tag{3.7}$$

where W_{mn}^α, Ψ_{mn}^α and Φ_{mn}^α are arbitrary parameters. The function $X(\lambda_m x)$ can be constructed for any combination of boundary conditions at the edges $x = 0, a$. The forms of $X(\lambda_m x)$ and the corresponding values of λ_m for SS, CC, CS, and CF plates are defined in the Appendix, see also [21].

For a SS boundary condition, the uniformly distributed load is expressed in terms of a Fourier series (Navier's solution). With a total of N terms in both the x and the y directions the uniformly distributed load $f(x, y)$ is expressed directly as

$$f(x, y) = \sum_{m=1}^{N} \sum_{n=1}^{N} F_{mn} \sin \frac{m\pi x}{a} \sin \frac{n\pi y}{b}, \tag{3.8}$$

in which the coefficients F_{mn} are defined as follows:

$$F_{mn} = \frac{16 f_0}{mn\pi^2} \begin{cases} 1 & \text{if } m, n = 1, 3, 5, \ldots, N, \\ 0 & \text{otherwise.} \end{cases} \tag{3.9}$$

For a sinusoidally distributed load, we have $m = n = 1$ and $F_{11} = f_0$.

Once again, substitution of Equations (2.1), (2.3), (2.4), (2.9), (2.10), and (2.13) considered in conjunction with (3.4) and (3.5) in the variational formulations (2.7) and (2.8) yields a system of algebraic equations expressed in a compact form according to the three problems as:

Free vibration problem ($S_1 = S_2 = f = 0$):

$$\left([L] - \omega^2[R]\right)\{\Delta\} = \{0\}. \tag{3.10}$$

Static buckling problem ($\omega \to 0$ in Equation (3.4), $S_1 = -\beta$, $S_2 = -\gamma\beta$, $f = 0$):

$$([L] - \beta[S])\{\Delta\} = \{0\}. \tag{3.11}$$

Bending problem ($\omega \to 0$ in Equation (3.4), $S_1 = S_2 = 0$):

$$[L]\{\Delta\} = \{F\}. \tag{3.12}$$

For all problems $\{\Delta\}$ denotes the column

$$\{\Delta\}^{\mathrm{T}} = \{W^{\alpha}_{mn}, \Psi^{\alpha}_{mn}, \Phi^{\alpha}_{mn}\}, \tag{3.13}$$

and for bending problem $\{F\}$ denotes the column

$$\{F\}^{\mathrm{T}} = \{-F_{mn}\xi_0, 0, 0\}, \tag{3.14}$$

where ξ_0 for a *SS* boundary condition is given by

$$\xi_0 = \int_0^a \sin^2 \frac{m\pi x}{a}\, \mathrm{d}x = \frac{a}{2}, \tag{3.15}$$

while for other boundary conditions it is given by

$$\xi_0 = \int_0^a X(\lambda_m x)\, \mathrm{d}x. \tag{3.16}$$

The elements of the symmetric matrices $[L]$, $[R]$ and $[S]$ are expressed as:

$$\begin{aligned} &L_{11} = \lambda_m^2 A^{\alpha}_{55}\xi_2 + \mu_n^2 A^{\alpha}_{44}\xi_1, \quad L_{12} = \lambda_m A^{\alpha}_{55}\xi_2, \\ &L_{13} = \mu_n A^{\alpha}_{44}\xi_1, \quad L_{22} = \lambda_m^2 D^{\alpha}_{11}\xi_3 + \mu_n^2 D^{\alpha}_{66}\xi_2 + A^{\alpha}_{55}\xi_2, \\ &L_{23} = \lambda_m\mu_n(D^{\alpha}_{66}\xi_2 - D^{\alpha}_{12}\xi_4), \quad L_{33} = \lambda_m^2 D^{\alpha}_{66}\xi_2 + \mu_n^2 D^{\alpha}_{22}\xi_1 + A^{\alpha}_{44}\xi_1; \end{aligned} \tag{3.17}$$

$$R_{11} = \rho h\xi_1, \quad R_{22} = \rho\frac{h^3}{12}\xi_2, \quad R_{33} = \rho\frac{h^3}{12}\xi_1, \quad R_{12} = R_{13} = R_{23} = 0; \tag{3.18}$$

$$S_{11} = \lambda_m^2\xi_2 + \gamma\mu_n^2\xi_1, \quad S_{12} = S_{13} = S_{22} = S_{23} = S_{33} = 0, \tag{3.19}$$

where

$$\begin{aligned} &\xi_1 = \int_0^a [X(\lambda_m x)]^2\, \mathrm{d}x, \quad \xi_2 = \int_0^a [X'(\lambda_m x)]^2\, \mathrm{d}x, \\ &\xi_3 = \int_0^a [X''(\lambda_m x)]^2\, \mathrm{d}x, \quad \xi_4 = \int_0^a X(\lambda_m x)X''(\lambda_m x)\, \mathrm{d}x, \end{aligned} \tag{3.20}$$

in which $(\,)'$ denotes differentiation with respect to $\overline{x}(\equiv \lambda_m x)$. Note that the functions $X(\lambda_m x)$ are normalized and then the outcomes of the integrals given in (3.20) are independent of m.

For non-trivial solutions of Equations (3.10) and (3.11), the following determinants should be zero,

$$\big|[L] - \omega^2[R]\big| = 0, \quad \big|[L] - \beta[S]\big| = 0. \tag{3.21}$$

The above equations yield the eigenfrequencies ω and critical buckling loads β. For bending problem, one needs to solve the 3×3 matrix equation (3.12) for the vector of amplitudes of the generalized displacements.

4. Discussion of the results

In order to put into evidence the influence of shear deformations and orthotropic material characteristics, we shall consider several numerical applications. These will be done for the case of the orthotropic material:

$$E_1 = 20{\cdot}83 \text{ Msi}, \quad E_2 = 10{\cdot}94 \text{ Msi}, \quad E_3 = 10{\cdot}00 \text{ Msi}, \quad v_{12} = v_{13} = 0{\cdot}44,$$

$$G_{12} = 6{\cdot}10 \text{ Msi}, \quad G_{13} = 3{\cdot}71 \text{ Msi}, \quad G_{23} = 6{\cdot}19 \text{ Msi}, \quad v_{32} = 0{\cdot}23. \tag{4.1}$$

The numerical applications are done, unless otherwise stated, by use of MFPT for homogeneous flat plates with various boundary conditions. The designation SS, CC, CS, and CF refer to the edge conditions associated to $x = 0, a$, only. The edges $y = 0, b$ are invariably assumed to be simply-supported. The following normalization is used in the comparison of all the numerical results ($\overline{z} = z/h$):

$$\begin{aligned}
&\overline{\omega} = \omega h\sqrt{\frac{\rho}{c_{11}}}, \quad \overline{\beta} = \frac{\beta a^2}{h^3 E_1}, \quad \overline{w} = -w^{\alpha}\left(\frac{a}{2}, \frac{b}{2}, \right)\frac{c_{11}}{hf_0},\\
&\overline{\sigma}_{11} = -\sigma_{11}^{\alpha}\left(\frac{a}{2}, \frac{b}{2}, \overline{z}\right)\frac{1}{f_0}, \quad \overline{\sigma}_{22} = -\sigma_{22}^{\alpha}\left(\frac{a}{2}, \frac{b}{2}, \overline{z}\right)\frac{1}{f_0},\\
&\overline{\sigma}_{12} = \sigma_{12}^{\alpha}(0, 0, \overline{z})\frac{1}{f_0}, \quad \overline{\sigma}_{23} = -\sigma_{23}^{\alpha}\left(\frac{a}{2}, 0, \overline{z}\right)\frac{1}{f_0}, \quad \overline{\sigma}_{13} = -\sigma_{13}^{\alpha}\left(0, \frac{b}{2}, \overline{z}\right)\frac{1}{f_0}.
\end{aligned} \tag{4.2}$$

To demonstrate the accuracy of the MFPT, comparisons between the data computed here and those in [14–17] have been made in Tables 1–8 and Figures 2–4. Results in [17] are based on the exact three-dimensional elasticity solutions of Srinivas and Rao for simply-supported rectangular plates. The results obtained in [15] as per the higher-order shear deformation theory (HSDT) developed by Reddy and in [16] as per the theory referred to as DT developed by Librescu *et al.*, are used to assess the improvement in the prediction of natural frequencies and critical buckling loads. The deflections and stresses for a single-layer orthotropic plate are obtained here according to the equations listed in [14] as per HSDT developed by Reddy.

As seen in Tables 1 and 2, the present results obtained by means of MFPT are found to be in good agreement with their counterparts available in the field literature, obtained for SS edge conditions. Note that the MFPT does not require additional higher-order stress resultants and material stiffness coefficients as used in the HSDT and DT. For SFPT solutions, one needs a value of the shear correction factor k. Two commonly used values of the factor are 5/6 from Reissner's work [5] and $\pi^2/12$ from Mindlin's work [6]. The results of SFPT based on these two and other shear-correction factor values are also included in Tables 1 and 2. They are in good agreement with the results of other investigators. SFPT could provide more reliable results in the case of $k = 5/6$ and $\pi^2/12$. In fact, MFPT yields identical frequencies and critical buckling loads with SFPT in which framework the transverse shear correction factor $k(= 5/6)$ is to be incorporated.

A comparison with the deflections and stresses of Reddy [14] is presented in Table 3. It is considered that the plate is made by a single orthotropic layer and subjected to a sinusoidal distributed load. It can be seen that there is excellent agreement between the MFPT results and the results of HSDT. The first four significant digits coincide for the center-point deflection. The first three significant digits coincide for the transverse shear stresses. Only minor deviation in the in-plane stresses is observed.

The results of our calculations for different N-term series are presented in Table 4 along with the data from Srinivas and Rao [17] and the obtained results from Reddy [14]. It is to be concluded that, accounting for round-off accuracy, the present MFPT provides more accurate results with the exact solution when $N = 25$. It is also seen that the present deflections are

Table 1. Natural frequencies $\overline{\omega}$ of SS orthotropic square plates.

m	n	Exact[a]	HSDT[b]	DT[c]	MFPT[d]	SFPT[d]			
						$k=1$	$=\frac{3}{4}$	$k=\frac{\pi^2}{12}$	$k=\frac{5}{6}$
1	1	0·0474	0·0474	0·0474	0·0474	0·0477	0·0472	0·0474	0·0474
1	2	0·1033	0·1033	0·1032	0·1032	0·1042	0·1025	0·1031	0·1032
2	1	0·1188	0·1189	0·1187	0·1187	0·1207	0·1174	0·1185	0·1187
2	2	0·1694	0·1695	0·1692	0·1691	0·1724	0·1670	0·1688	0·1691
1	3	0·1888	0·1888	0·1884	0·1883	0·1910	0·1865	0·1880	0·1883
3	1	0·2180	0·2184	0·2177	0·2175	0·2240	0·2135	0·2170	0·2175
2	3	0·2475	0·2477	0·2469	0·2465	0·2522	0·2429	0·2461	0·2465
3	2	0·2624	0·2629	0·2619	0·2614	0·2695	0·2564	0·2608	0·2614
1	4	0·2969	0·2969	0·2958	0·2949	0·3010	0·2911	0·2945	0·2949
4	1	0·3319	0·3330	0·3310	0·3299	0·3436	0·3217	0·3289	0·3290
3	3	0·3320	0·3326	0·3310	0·3297	0·3406	0·3230	0·3289	0·3297
2	4	0·3476	0·3479	0·3462	0·3446	0·3540	0·3387	0·3438	0·3446
4	2	0·3670	0·3720	0·3695	0·3677	0·3831	0·3584	0·3665	0·3677

[a]Results obtained in [17] using the 3D-elasticity theory.
[b]Results reported in [15] using HSDT.
[c]Results reported in [16] using DT.
[d]Results obtained in this paper.

Table 2. Non-dimensional critical buckling loads $\overline{\beta}$ of SS orthotropic square plates.

γ	a/h	HSDT[a]	DT[b]	MFPT[c]	SFPT[c]			
					$k=1$	$k=\frac{3}{4}$	$k=\frac{\pi^2}{12}$	$k=\frac{5}{6}$
0·0	2	0·9581	0·9435	0·9436	1·0561	0·8815	0·9358	0·9436
	5	2·0999	2·0978	2·0984	2·1871	2·0433	2·0917	2·0984
	10	2·5706	2·5704	2·5712	2·6041	2·5497	2·5686	2·5712
	20	2·7258	2·7258	2·7267	2·7359	2·7206	2·7260	2·7267
	50	2·7729	2·7729	2·7729	2·7754	2·7728	2·7737	2·7729
0·5	2	0·6388	0·6290	0·6291	0·7041	0·5877	0·6238	0·6291
	5	1·3999	1·3986	1·3989	1·4581	1·3622	1·3944	1·3989
	10	1·7137	1·7136	1·7141	1·7361	1·6998	1·7124	1·7141
	20	1·8172	1·8172	1·8178	1·8239	1·8137	1·8173	1·8178
	50	1·8486	1·8486	1·8492	1·8502	1·8485	1·8491	1·8492
1·0	2	0·4791	0·4718	0·4781	0·5280	0·4407	0·4678	0·4781
	5	1·0500	1·0489	1·0492	1·0936	1·0216	1·0458	1·0492
	10	1·2853	1·2852	1·2856	1·3021	1·2749	1·2843	1·2856
	20	1·3629	1·3629	1·3633	1·3680	1·3603	1·3630	1·3633
	50	1·3864	1·3864	1·3869	1·3877	1·3864	1·3869	1·3869

[a]Results reported in [15] using HSDT.
[b]Results reported in [16] using DT.
[c]Results obtained in this paper.

Table 3. Non-dimensional deflections and stresses of *SS* orthotropic plates under sinusoidal load.

a/b	h/a	$\overline{w}$		$\overline{\sigma}_{11}(\overline{z}=0{\cdot}5)$		$\overline{\sigma}_{22}(\overline{z}=0{\cdot}5)$	
		HSPT[a]	MFPT[b]	HSPT	MFPT	HSPT	MFPT
0·5	0·05	14198·7	14198·7	182·590	182·050	62·7165	62·5639
	0·10	931·165	931·212	45·9116	45·3726	15·8891	15·7366
	0·14	256·919	256·967	23·5978	23·0599	8·2423	8·0899
1·0	0·05	6618·35	6618·38	98·5339	98·1367	60·9192	60·7528
	0·10	438·631	438·665	24·6735	24·2783	15·5374	15·3711
	0·14	122·441	122·475	12·6193	12·2264	8·1232	7·9571
2·0	0·05	1320·27	1320·29	30·2167	29·9910	37·0668	36·8838
	0·10	90·9455	90·9656	7·5275	7·3051	9·5493	9·3665
	0·14	26·4377	26·4574	3·8333	3·6147	5·0462	4·8637

[a]Results obtained in [14] using HSDT.
[b]Results obtained in this paper using MFPT.

Table 3. (continued).

a/b	h/a	$\overline{\sigma}_{23}(\overline{z}=0{\cdot}0)$		$\overline{\sigma}_{13}(\overline{z}=0{\cdot}0)$		$\overline{\sigma}_{12}(\overline{z}=0{\cdot}5)$	
		HSPT	MFPT	HSPT	MFPT	HSPT	MFPT
0·5	0·05	3·0139	3·0144	8·0404	8·0421	45·3295	45·4800
	0·10	1·5191	1·5201	4·0113	4·0146	11·3352	11·4860
	0·14	1·0958	1·0973	2·8572	2·8618	5·7832	5·9343
1·0	0·05	4·0398	4·0406	5·5072	5·5087	41·9359	42·1407
	0·10	2·0358	2·0375	2·7342	2·7371	10·3673	10·5716
	0·14	1·4681	1·4705	1·9359	1·9399	5·2128	5·4166
2·0	0·05	3·5399	3·5413	2·4654	2·4667	16·2291	16·4111
	0·10	1·7831	1·7859	1·2004	1·2029	3·8265	4·0054
	0·14	1·2841	1·2880	0·8311	0·8344	1·8115	1·9868

very close to the corresponding ones of HSDT developed by Reddy [14]. In addition, Figure 2 shows the plots of nondimensional stresses *vs.* side-to-thickness ratio for a square plate under uniformly distributed load (with 25-term series). The variations of all stresses calculated in the present analysis and in Reddy [14] have been compared. The in-plane stresses are calculated at $\overline{z}=0{\cdot}5$, while the transverse shear stresses are calculated at $\overline{z}=0$. It can be seen that there is an excellent agreement between the results for all side-to-thickness ratios.

The next example provides a comparison of MFPT with the SFPT solutions based on various shear-correction factors for plates subjected to uniformly distributed loading with 25-term series. In Tables 5–8, as mentioned before, MFPT yields identical deflections and in-plane stresses with SFPT in which framework the transverse shear correction factor $k(=5/6)$ is to be incorporated. It yields very close transverse shear stresses with SFPT in which framework the transverse shear correction factor $k(=2/3)$ is to be incorporated.

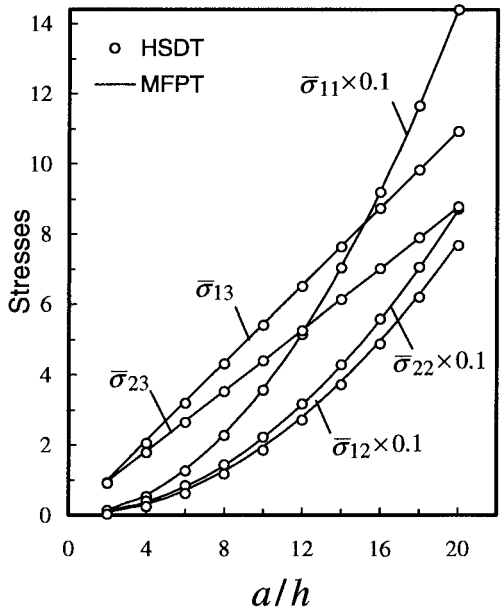

Figure 2. Nondimensional stresses *vs.* side-to-thickness ratio (a/h) for a square plate subjected to uniform distributed load.

Table 4. Non-dimensional deflections of *SS* orthotropic plates under uniform load.

a/b	h/a	Exact[a]	HSPT[b]				MFPT[c]			
			N[d] $= 9$	$N = 19$	$N = 25$	$N = 45$	$N = 9$	$N = 19$	$N = 25$	$N = 45$
0·5	0·05	21542	21543·3	21539·1	21539·4	21539·3	21543·4	21539·1	21539·4	21539·3
	0·10	1408·5	1409·0	1408·6	1408·7	1408·7	1409·1	1408·7	1408·7	1408·7
	0·14	387·23	387·58	387·43	387·45	387·45	387·63	387·48	387·50	387·50
1·0	0·05	10443	10444·3	10443·6	10443·7	10443·7	10444·3	10443·7	10443·7	10443·7
	0·10	688·57	689·41	689·31	689·33	689·32	689·45	689·35	689·36	689·36
	0·14	191·07	191·59	191·54	191·55	191·55	191·62	191·58	191·58	191·58
2·0	0·05	2048·7	2050·9	2050·5	2050·6	2050·6	2050·9	2050·9	2050·6	2050·6
	0·10	139·08	139·82	139·76	139·77	139·77	139·84	139·78	139·79	139·78
	0·14	39·79	40·22	40·19	40·20	40·20	40·24	40·21	40·21	40·21

[a]Results obtained in [17] using the 3D-elasticity theory.
[b]Results obtained in [14] using HSDT.
[c]Results obtained in this paper using MFPT.
[d]$N \times N$-term series.

In Figures 3 and 4 the through-the-thickness variations of in-plane normal stress $\sigma_{11}^{*}[= \sigma_{11}(\overline{z})/\sigma_{11}(0{\cdot}5)]$ and the transverse shear stress $\sigma_{13}^{*}[= \sigma_{13}(\overline{z})/\sigma_{13}(0)]$ calculated in the present analysis and in Srinivas and Rao [17] are compared. There is an excellent agreement between the results due to the exact elasticity solution and the present solutions of MFPT and SFPT (with any shear correction factor k). Unlike in the traditional SFPT, the distribution of transverse shear stress σ_{13}^{*} due to MFPT is not uniform through-the-thickness, instead it takes the same form as in the exact elasticity solution.

Table 5. Comparison of the center deflections $\overline{w}$ of SS orthotropic flat plates.

a/b	h/a	Exact[a]	MFPT[b]	SFPT[b]				
				$k=1$	$k=\frac{2}{3}$	$k=\frac{3}{4}$	$k=\frac{\pi^2}{12}$	$k=\frac{5}{6}$
0·5	0·05	21542	21539·4	21483·8	21622·8	21576·5	21543·8	21539·4
	0·10	1408·5	1408·7	1394·83	1429·54	1417·97	1409·82	1408·7
	0·14	387·23	387·50	380·43	398·11	392·22	388·06	387·50
1·0	0·05	10443	10443·7	10411·1	10492·7	10465·5	10446·3	10443·7
	0·10	688·57	689·36	681·24	701·53	694·77	690·00	689·36
	0·14	191·07	191·58	187·46	197·75	194·33	191·91	191·58
2·0	0·05	2048·7	2050·6	2040·2	2066·2	2057·5	2051·4	2050·6
	0·10	139·08	139·79	137·21	143·63	141·50	139·99	139·79
	0·14	39·79	40·21	38·92	42·15	41·07	40·32	40·21

[a]Results obtained in [17] using the 3D-elasticity theory.
[b]Results obtained in this paper.

Table 6. Comparison of the in-plane normal stress $\overline{\sigma}_{11}(\overline{z}=0{\cdot}5)$ of SS orthotropic flat plates.

a/b	h/a	Exact[a]	MFPT[b]	SFPT[b]				
				$k=1$	$k=\frac{2}{3}$	$k=\frac{3}{4}$	$k=\frac{\pi^2}{12}$	$k=\frac{5}{6}$
0·5	0·05	262·67	262·10	262·13	262·06	262·08	262·099	262·10
	0·10	65·975	65·396	65·425	65·353	65·377	65·394	65·396
	0·14	33·862	33·281	33·310	33·238	33·262	33·279	33·281
1·0	0·05	144·31	143·90	143·98	143·78	143·84	143·890	143·90
	0·10	36·021	35·619	35·697	35·502	35·567	35·613	35·619
	0·14	18·346	17·947	18·023	17·833	17·896	17·941	17·974
2·0	0·05	40·657	40·511	40·566	40·428	40·474	40·5064	40·511
	0·10	10·025	9·8895	9·9408	9·8142	9·8557	9·8854	9·8895
	0·14	5·0364	4·9035	4·9503	4·8362	4·8732	4·8998	4·9035

[a]Results obtained in [17] using the 3D-elasticity theory.
[b]Results obtained in this paper.

Now, we restrict our attention to the bending problem of a single-layer orthotropic plate under a uniformly distributed loading with a 25-term series. The obtained results concern the values of the nondimensional deflections and stresses displayed in Table 9 using MFPT for various edge conditions while the Figures 5–8 depict the variation of the same quantities *vs.* the geometrical parameters of the plate. Note that the following normalizations are used in Table 9 and Figures 5–10:

$$\hat{w} = -w^{\alpha}\left(\frac{a}{2},\frac{b}{2}\right)\frac{c_{11}h^2}{a^3 f_0}, \quad \hat{\sigma}_{11} = \sigma_{11}^{\alpha}\left(\frac{a}{2},\frac{b}{2},-\frac{h}{2}\right)\frac{h}{af_0}, \quad \hat{\sigma}_{22} = \sigma_{22}^{\alpha}\left(\frac{a}{2},\frac{b}{2},-\frac{h}{2}\right)\frac{h}{af_0},$$

$$\hat{\sigma}_{12} = \sigma_{12}^{\alpha}\left(\frac{a}{2},\frac{b}{2},\frac{h}{2}\right)\frac{h}{af_0}, \quad \hat{\sigma}_{13} = -\sigma_{13}^{\alpha}\left(0,\frac{b}{2},0\right)\frac{1}{f_0}, \quad \hat{\sigma}_{23} = -\sigma_{23}^{\alpha}\left(\frac{a}{2},0,0\right)\frac{1}{f_0}. \tag{4.3}$$

Table 7. Comparison of the in-plane normal stress $\overline{\sigma}_{22}(\overline{z}=0{\cdot}5)$ of SS orthotropic flat plates.

a/b	h/a	Exact[a]	MFPT[b]	SFPT[b]				
				$k=1$	$k=\frac{2}{3}$	$k=\frac{3}{4}$	$k=\frac{\pi^2}{12}$	$k=\frac{5}{6}$
0·5	0·05	79·545	79·238	79·219	79·266	79·250	79·240	79·238
	0·10	20·204	19·893	19·874	19·921	19·905	19·894	19·893
	0·14	10·515	10·204	10·185	10·232	10·216	10·206	10·204
1·0	0·05	87·080	86·837	86·781	86·922	86·875	86·842	86·837
	0·10	22·210	21·962	21·906	22·045	21·999	21·966	21·962
	0·14	11·615	11·366	11·312	11·447	11·402	11·370	11·366
2·0	0·05	54·279	54·106	54·063	54·169	54·134	54·109	54·106
	0·10	13·888	13·711	13·672	13·769	13·737	13·714	13·711
	0·14	7·2794	7·1048	7·0687	7·1566	7·1281	7·1076	7·1048

[a]Results obtained in [17] using the 3D-elasticity theory.
[b]Results obtained in this paper.

Table 8. Comparison of the transverse shear stress $\overline{\sigma}_{13}(\overline{z}=0{\cdot}0)$ of SS orthotropic flat plates.

a/b	h/a	Exact[a]	MFPT[b]	SFPT[b]				
				$k=1$	$k=\frac{2}{3}$	$k=\frac{3}{4}$	$k=\frac{\pi^2}{12}$	$k=\frac{5}{6}$
0·5	0·05	14·048	14·104	9·4031	14·103	12·537	11·432	11·283
	0·10	6·9266	7·0481	4·6992	7·0470	9·2645	5·7129	5·6385
	0·14	4·8782	5·0315	3·3549	5·0300	4·4718	4·0783	4·0252
1·0	0·05	10·873	10·955	7·3049	10·953	9·7370	8·8800	8·7643
	0·10	5·3411	5·4608	3·6430	5·4552	4·8515	4·4261	4·3687
	0·14	3·7313	3·8849	2·5935	3·8767	3·4500	3·1486	3·1079
2·0	0·05	6·2434	6·2560	4·1742	6·2482	5·5578	5·0706	5·0048
	0·10	2·9570	3·0801	2·0605	3·0640	2·7315	2·4959	2·4640
	0·14	1·9887	2·1568	1·4475	2·1360	1·9088	1·7474	1·7255

[a]Results obtained in [17] using the 3D-elasticity theory.
[b]Results obtained in this paper.

Figures 5 and 6 reveal that the variation of $\hat{w}$ is very sensitive to the variations of a/h and a/b parameters and this depending on the considered boundary conditions. In this sense the CF instance shows the highest sensitivity in the context of the considered edge conditions for square and moderately thick rectangular plates.

In Figure 7, the obtained results of $\hat{\sigma}_{13}$ for a SS square plate using MFPT and SFPT with various shear-correction factors are compared. The SFPT gives an identical value with MFPT only at $\overline{z}=0$ and when the shearing-correction factor is assumed to be 2/3. Figure 8 reveals also the sensitivity of $\hat{\sigma}_{23}$ through the thickness of the square plate for various edge conditions.

Finally, Figures 9 and 10 display the variation of $\hat{w}$ and $\hat{\sigma}_{23}$ *vs.* the assumed values of shear-correction factor k for various edge conditions. They reveal that the results of MFPT are independent of the shear-correction factor, while the results predicted by SFPT strongly depend on the proper selection of the transverse shear-correction factor and that in this depen-

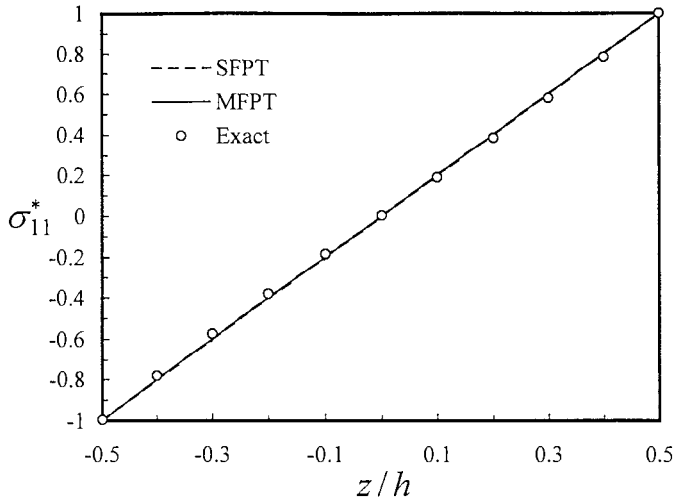

Figure 3. Comparison of the distribution of in-plane normal stress (σ_{11}^*) through-the-thickness of a SS square plate ($h/a = 0{\cdot}14$).

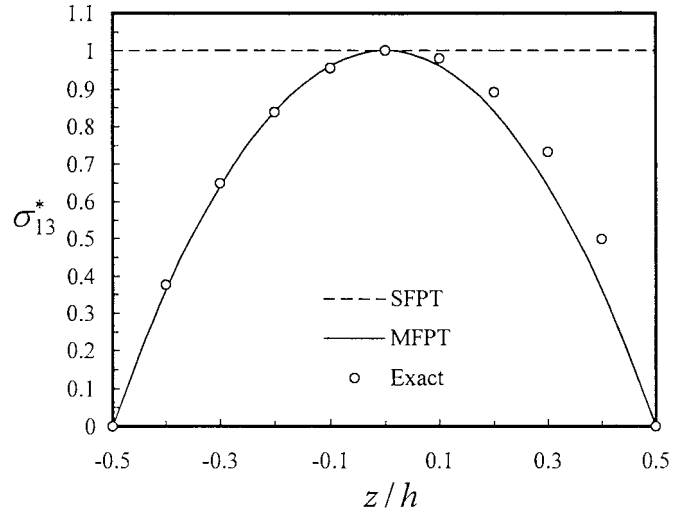

Figure 4. Comparison of the distribution of transverse shear stress (σ_{13}^*) through-the-thickness of a SS square plate ($h/a = 0{\cdot}14$).

dence also the character of boundary conditions is involved. Increasing k results in a decrease of the nondimensional center deflection ($\hat{w}$). However, for the transverse shear stress ($\hat{\sigma}_{23}$), the effect of the shear-correction factor is more significant.

The SFPT deflections with shear correction factor of 5/6 are very close of the MFPT values for all four types of plate configurations (see Figure 9). Most interestingly, it is noted from Figures 7 and 10 that, in all the cases, the SFPT shear stresses with shear correction factor of 2/3 match most closely with the MFPT values (see also Table 8).

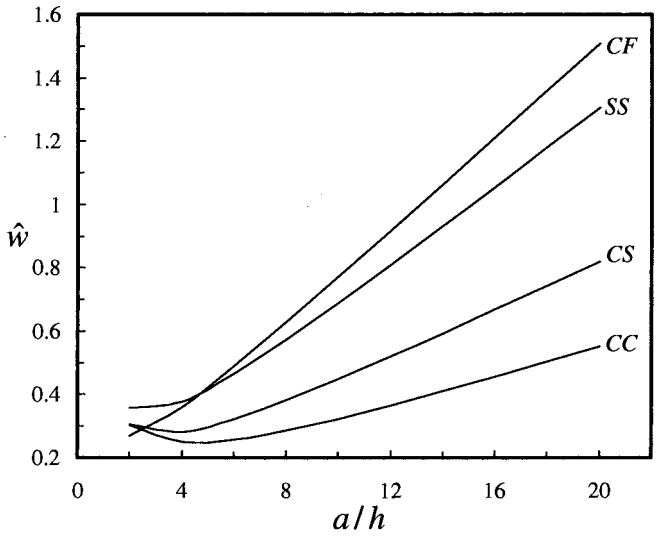

Figure 5. Nondimensional center deflection ($\hat{w}$) *vs.* side-to-thickness ratio (a/h) for a square plate.

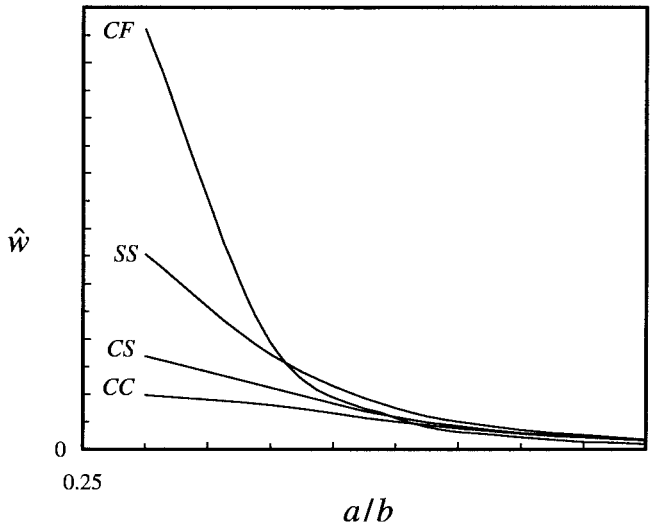

Figure 6. Nondimensional center deflection ($\hat{w}$) *vs.* aspect ratio (a/b) for a rectangular plate ($a/h = 10$).

5. Conclusions

The simple and mixed variational formulations are used to develop both the analytical and numerical solutions for the state of stress of anisotropic elastic plates based on Reissner-Mindlin's thick-plate theory. The plate is considered as a single layer of orthotropic material and subjected to a distributed transverse load as well as in-plane edge forces. Numerical results are presented for natural frequencies, critical loads, deflections, and stresses of rectangular plates exhibiting various edge conditions. Comparisons are made to show that the results obtained using the present theories are in close agreement with the available exact and higher-order shear deformation theory solutions in the literature. The results of MFPT and SFPT themselves are compared to show the effect of the shear correction factors. Both MFPT and

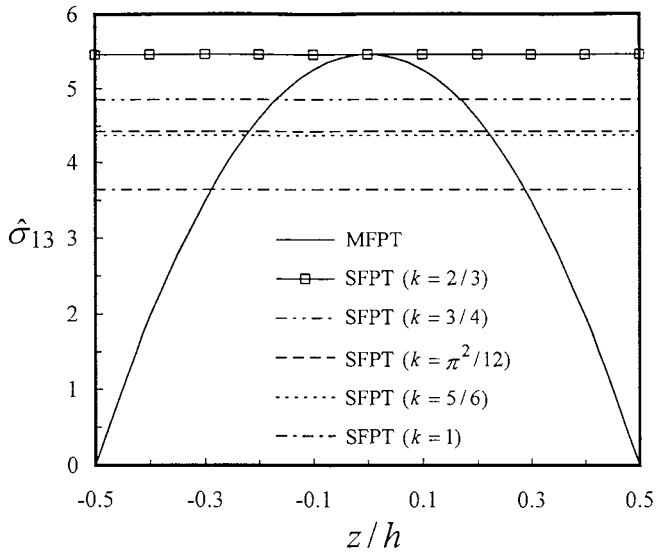

Figure 7. Variation of the transverse shear stress ($\hat{\sigma}_{13}$) through-the-thickness of a SS square plate using MFPT and SFPT with various shear correction factors ($a/h = 10$).

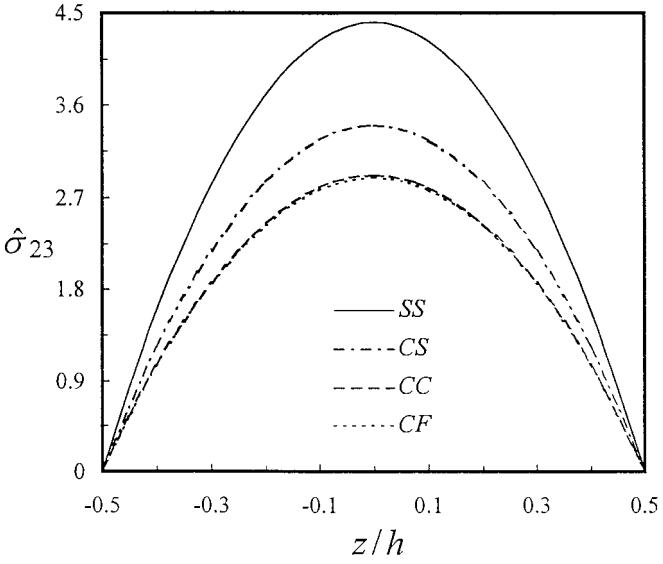

Figure 8. Variation of the transverse shear stress ($\hat{\sigma}_{23}$) through-the-thickness of a square plate ($a/h = 10$).

SFPT (with a proper shear-correction factor) allow one to treat the global structural behaviour of homogeneous plates for a variety of boundary conditions. In general, SFPT predicts deflections and in-plane stresses that are significantly different from those of MFPT, even if the transverse shear-correction factor (for SFPT) is assumed to be 5/6. This is more obvious when the transverse shear stresses obtained by use of the SFPT and MFPT are compared in which the appropriate shear-correction factor value for SFPT is assumed to be 2/3. So, the validity of the MFPT is demonstrated by applying it to solve vibration, buckling and bending problems of elastic plates for which exact results are available. The use of a mixed variational formulation enables the MFPT to account for variable distributions of transverse shear stresses, which

Table 9. Nondimenisional deflections and stresses of an orthotropic rectangular flat plate ($a/h = 10$).

a/b	BC	$\hat{w}$	$\hat{\sigma}_{11}$	$\hat{\sigma}_{22}$	$\hat{\sigma}_{13}$	$\hat{\sigma}_{23}$	$\hat{\sigma}_{12}$
0·5	*SS*	1·4087	6·5396	1·9893	7·0481	4·5816	2·4766
	CC	0·3935	2·5548	0·6239	–	2·7117	–
	CS	0·6775	3·6332	0·9855	–	3·2539	–
	CF	3·0402	−4·5107	0·4372	–	3·3886	–
1·0	*SS*	0·6894	3·5619	2·1962	5·4608	4·4067	1·9466
	CC	0·3232	2·2684	1·0888	–	2·9135	–
	CS	0·4489	2·6420	1·4574	–	3·3981	–
	CF	0·7724	−0·4944	1·5459	–	2·8956	–
2·0	*SS*	0·1398	0·9889	1·3710	3·0801	3·2746	0·7899
	CC	0·1148	1·0211	1·1612	–	2·9709	–
	CS	0·1209	0·9345	1·1970	–	2·9634	–
	CF	0·0875	0·2159	0·7771	–	1·8188	–

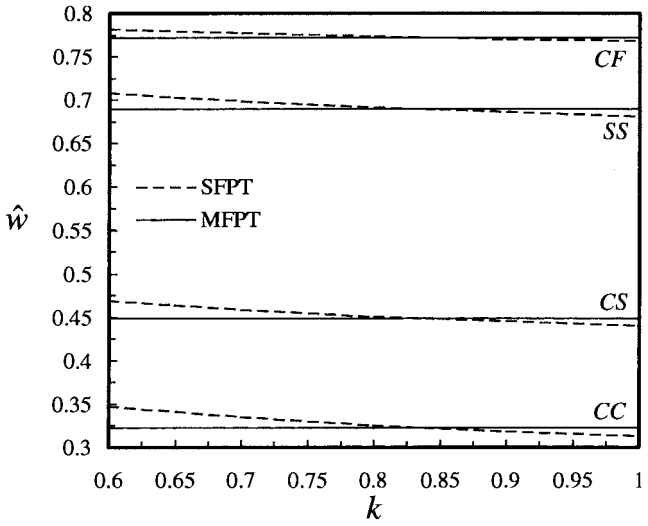

Figure 9. Effect of transverse shear correction factor (k) of SFPT on the nondimensional center deflection ($\hat{w}$) for a square plate ($a/h = 10$).

Reissner-Mindlin's traditional SFPT fails to do. Since a parabolic distribution for the shear stress is assumed, the MFPT does not require the use of any shear-correction factor used in other first-order theories. Also, it does not require additional stress resultants and material stiffness coefficients used in other higher-order theories.

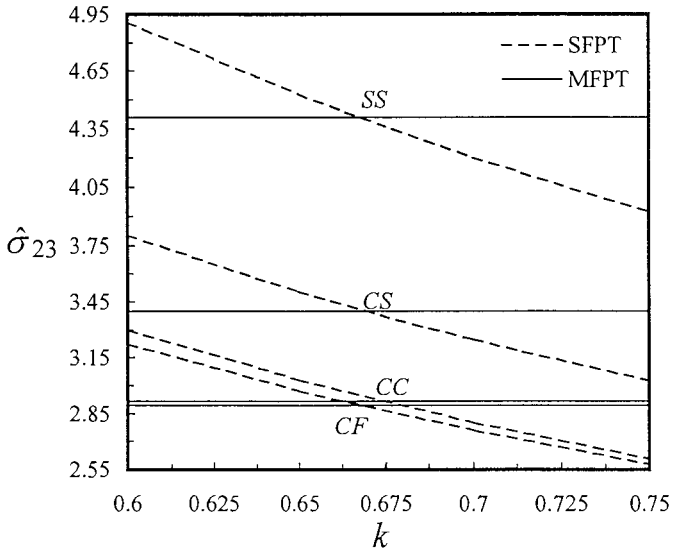

Figure 10. Effect of transverse shear correction factor (k) of SFPT on the transverse shear stress ($\hat{\sigma}_{23}$) for a square plate ($a/h = 10$).

Appendix

The forms of the function $X(\lambda_m x)$ are given by:

BC	$X(\lambda_m x)$	η_m
SS	$\sin \lambda_m x$	–
CC	$\sin \lambda_m x - \text{sh}\, \lambda_m x - \eta_m(\cos \lambda_m x - \text{ch}\, \lambda_m x)$	$(\text{sh}\overline{\lambda}_m - \sin \overline{\lambda}_m)/(\text{ch}\overline{\lambda}_m - \cos \overline{\lambda}_m)$
CS	$\sin \lambda_m x - \text{sh}\, \lambda_m x - \eta_m(\cos \lambda_m x - \text{ch}\lambda_m x)$	$(\text{sh}\overline{\lambda}_m + \sin \overline{\lambda}_m)/(\text{ch}\overline{\lambda}_m + \cos \overline{\lambda}_m)$
CF	$\sin \lambda_m x - \text{sh}\, \lambda_m x - \eta_m(\cos \lambda_m x - \text{ch}\, \lambda_m x)$	$\text{sh}\overline{\lambda}_m + \sin \overline{\lambda}_m)/(\text{ch}\overline{\lambda}_m + \cos \overline{\lambda}_m)$

The values of $\overline{\lambda}_m (= \lambda_m a)$ corresponding to the function $X(\lambda_m x)$ for various boundary conditions are given by:

	m				
BC	1	2	3	4	≥ 5
SS	3·142	6·283	9·425	12·566	$m\pi$
CC	4·730	7·853	10·996	14·137	$(m + 0{\cdot}50)\pi$
CS	3·927	7·069	10·210	13·352	$(m + 0{\cdot}25)\pi$
CF	1·875	4·694	7·855	10·996	$(m - 0{\cdot}50)\pi$

References

1. S.P. Timoshenko and S. Woinowski-Krieger, *Theory of Plates and Shells*. Singapore: McGraw-Hill (1959) 580 pp.
2. E. Reissner and Y. Stavsky, Bending and stretching of certain types of heterogeneous aelotropic elastic plates. *ASME J. Appl. Mech.* 28 (1961) 402–408.

3. J.M. Whitney, *Structural Analysis of Laminated Anisotropic Plates*. Lancaster, PA: Technomic (1987) 354 pp.
4. E. Reissner, On the theory of bending of elastic plates. *J. Math. Phys.* 23 (1944) 184–191.
5. E. Reissner, The effect of transverse shear deformation on the bending of elastic plates. *ASME J. Appl. Mech.* 12 (1945) 69–77.
6. R.D. Mindlin, Influence of rotatory inertia and shear on flexural motions of isotropic, elastic plates. *ASME J. Appl. Mech.* 18 (1951) 31–38.
7. E. Reissner, On transverse bending of plates, including the effects of transverse shear deformation. *Int. J. Solids Struct.* 11 (1975) 569–573.
8. P.C. Yang, C.R. Norris and Y. Stavsky, Elastic wave propagation in heterogeneous plates. *Int. J. Solids Struct.* 2 (1966) 665–684.
9. E. Reissner, Reflection on the theory of elastic plates. *Appl. Mech. Rev.* 38 (1985) 1453–1464.
10. A.K. Noor and W.S. Burton, Assessment of shear deformation theories for multilayered composite plates. *Appl. Mech. Rev.* 42 (1989) 1–13.
11. J.N. Reddy, A review of refined theories of laminated composites plates. *Shock Vib. Dig.* 22 (1990) 3–17.
12. J.M. Whitney and C.T. Sun, A higher order theory for extensional motion of laminated composites. *J. Sound Vib.* 30 (1973) 85–97.
13. K.H. Lo, R.H. Christensen and E.M. Wu, A high-order theory of plate deformation, Part 1: homogeneous plates; Part 2: laminated plates. *J. Appl. Mech.* 44 (1977) 663–676.
14. J.N. Reddy, A simple higher-order theory for laminated composite plates. *J. Appl. Mech.* 51 (1984) 745–752.
15. J.N. Reddy, A refined nonlinear theory of plates with transverse shear deformation. *Int. J. Solids Struct.* 20 (1984) 881–896.
16. L. Librescu, A.A. Khdeir and J.N. Reddy, Further results concerning the dynamic response of shear deformable elastic orthotropic plates. *ZAMM* 70 (1990) 23–33.
17. S. Srinivas and A.K. Rao, Bending, vibration and buckling of simply supported thick orthotropic rectangular plates and laminates. *Int. J. Solids Struct.* 6 (1970) 1463–1481.
18. N.J. Pagano, Exact solutions for composite laminates in cylindrical bending. *J. Compos. Mater.* 3 (1969) 398–411.
19. N.J. Pagano, Exact solutions for rectangular bi-directional composites and sandwich plates. *J. Compos. Mater.* 4 (1970) 20–34.
20. N.J. Pagano and S.J. Hatfield, Elastic behavior of multilayered bidirectional composites. *AIAA J.* 10 (1972) 931–933.
21. A.M. Zenkour, Buckling and free vibration of elastic plates using simple and mixed shear deformation theories. *Acta Mech.* 146 (2001) 183–197.
22. M.E. Fares, M.N.M. Allam and A.M. Zenkour, Hamilton's mixed variational formula for dynamical problems of anisotropic elastic bodies. *SM Arch.* 14 (1989) 103–114.
23. M.E. Fares and A.M. Zenkour, Mixed variational formula for the thermal bending of laminated plates. *J. Thermal Stresses* 22 (1999) 347–365.
24. A.M. Zenkour, Natural vibration analysis of symmetrical cross-ply laminated elastic plates using mixed variational formulation. *Eur. J. Mech. A/Solids* 19 (2000) 469–485.
25. A.M. Zenkour, Stress analysis of axisymmetric shear deformable cross-ply circular laminated cylindrical shells. *J. Eng. Math.* 40 (2001) 315–332.